Electronic Supplementary Material (ESI) for Inorganic Chemistry Frontiers.

Supporting Information

Assembly of chiral 3d-4f wheel-like cluster complexes with achiral ligands: single-molecule magnet behaviour and magnetocaloric effect

Cai-Ming Liu,[*,†] De-Qing Zhang,[†] Xiang Hao,[†] and Dao-Ben Zhu[†]

[†]*Beijing National Laboratory for Molecular Sciences, Center for Molecular Science, Key Laboratory of Organic Solids, Institute of Chemistry, CAS Research/Education Center for Excellence in Molecular Science, Chinese Academy of Sciences, Beijing 100190, China. E-mail: cmliu@iccas.ac.cn*

Table of Contents

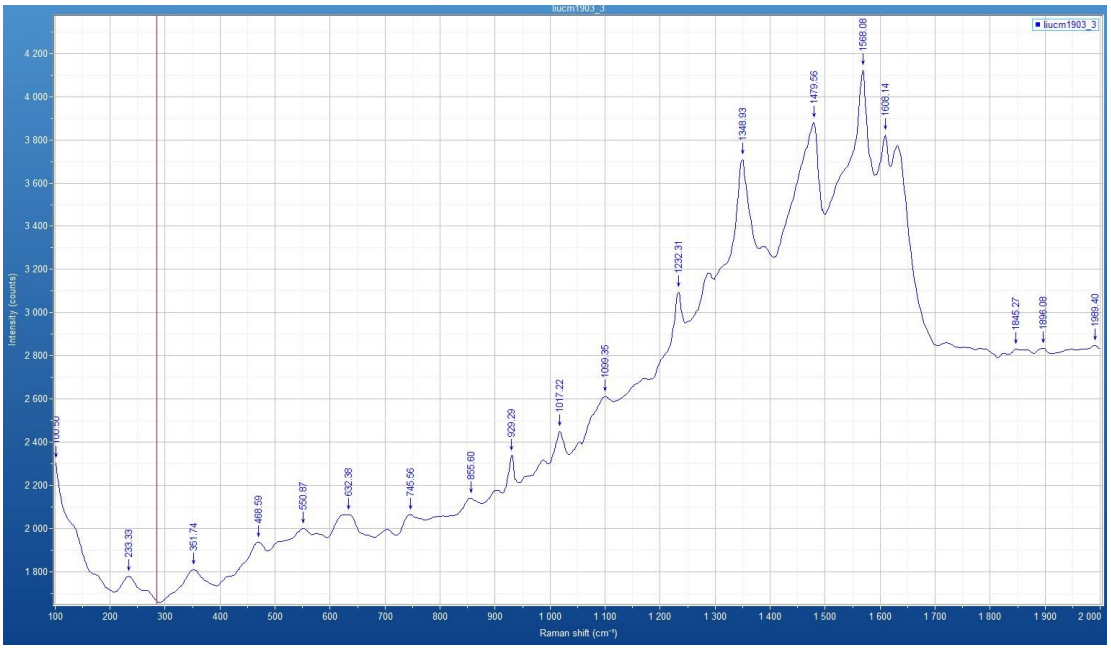

Fig. S1. Raman spectrum of complex **4**.

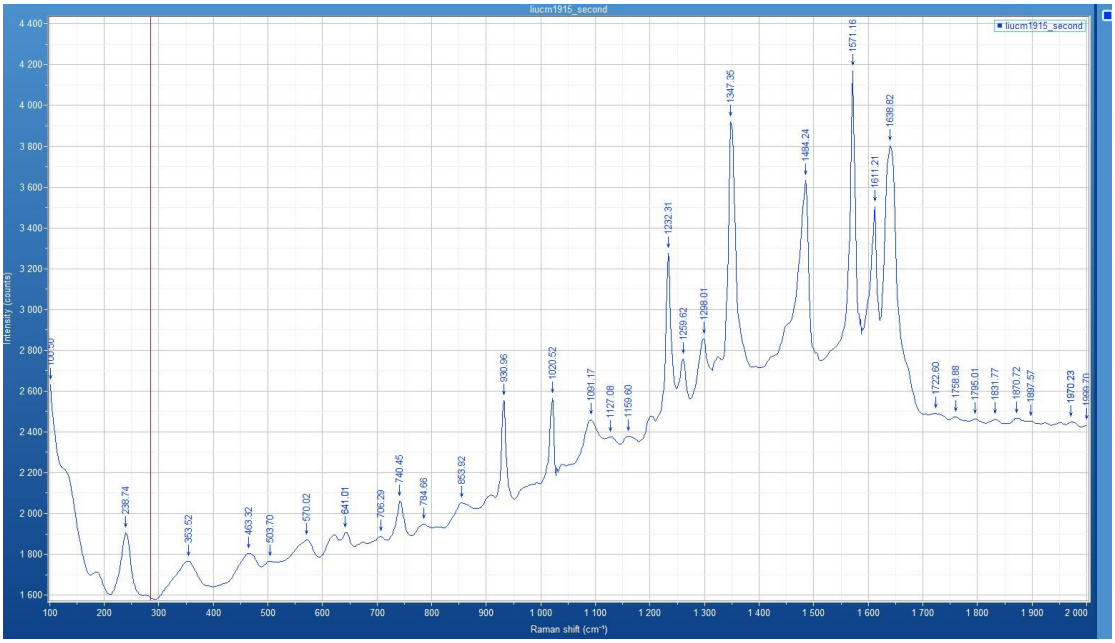

Fig. S2. Raman spectrum of complex **5**.

Table S1. Continuous Shape Measures calculation for Dy1 atom in **1-*S***.

Dy1 structures

EP-9	1 D9h	Enneagon
OPY-9	2 C8v	Octagonal pyramid
HBPY-9	3 D7h	Heptagonal bipyramid
JTC-9	4 C3v	Johnson triangular cupola J3
JCCU-9	5 C4v	Capped cube J8
CCU-9	6 C4v	Spherical-relaxed capped cube
JCSAPR-9	7 C4v	Capped square antiprism J10
CSAPR-9	8 C4v	Spherical capped square antiprism
JTCTPR-9	9 D3h	Tricapped trigonal prism J51
TCTPR-9	10 D3h	Spherical tricapped trigonal prism
JTDIC-9	11 C3v	Tridiminished icosahedron J63
HH-9	12 C2v	Hula-hoop
MFF-9	13 Cs	Muffin

Structure [ML9]	EP-9	OPY-9	HBPY-9	JTC-9	JCCU-9	CCU-9	JCSAPR-9	CSAPR-9	JTCTPR-9	TCTPR-9	JTDIC-9	HH-9	**MFF-9**
ABOXIY	33.661	22.181	17.376	16.003	10.464	8.748	5.007	4.357	6.627	5.073	13.344	7.153	**3.475**

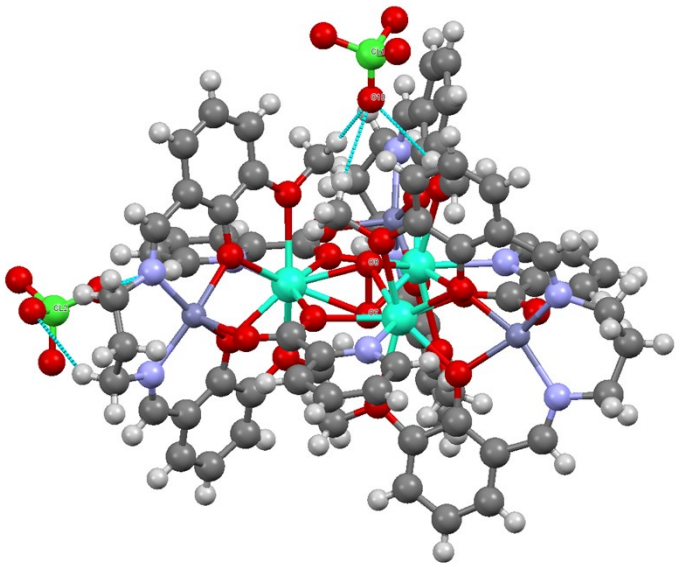

Fig. S3. Short contacts between the perchlorate anion and the $[Zn_3Dy_3(O_2)L_3(PyCO_2)_3]$ cation in **1-*S***.

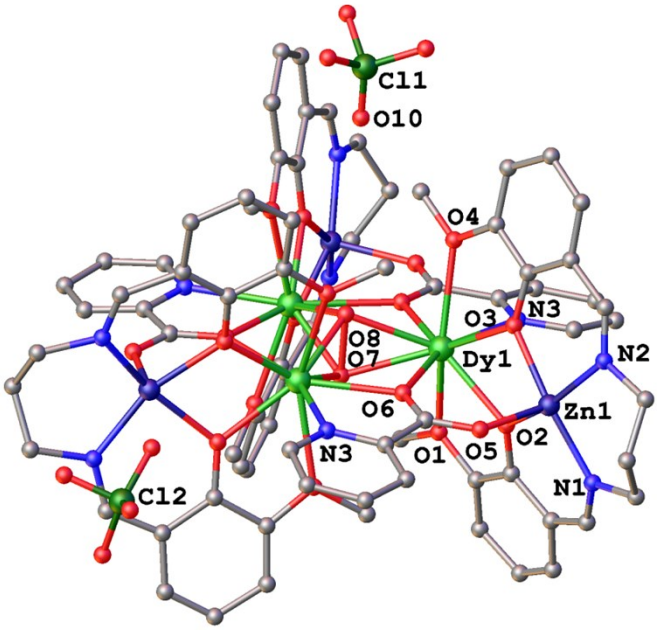

Fig. S4. Crystal structure of **1-*R***, H atoms, hydroxide anions and lattice hydrate molecules are not shown for clarity.

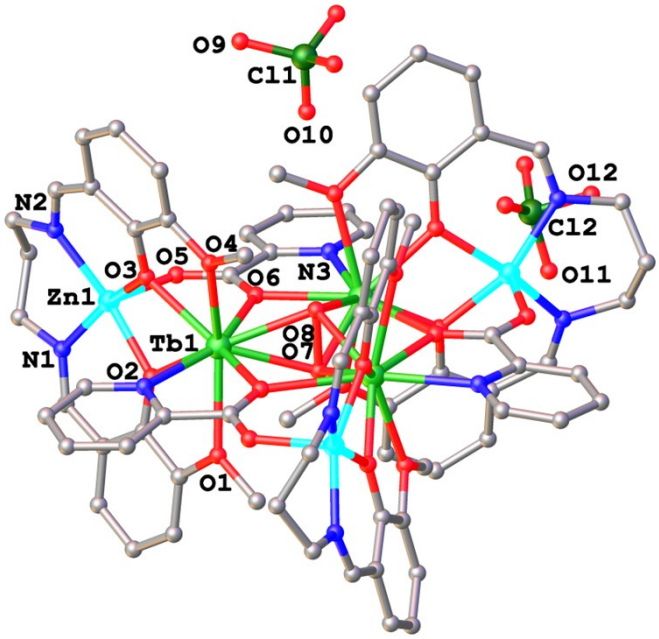

Fig. S5. Crystal structure of **2-*R***, H atoms, hydroxide anions and lattice hydrate molecules are not shown for clarity.

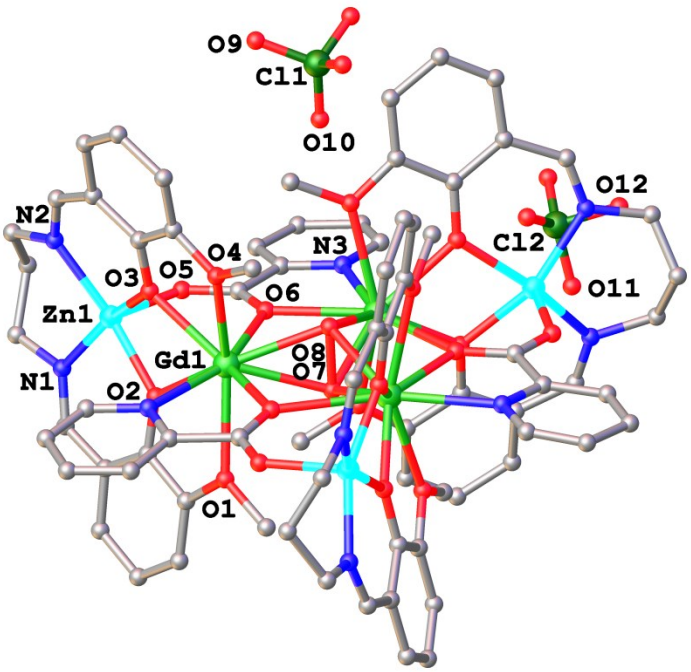

Fig. S6. Crystal structure of **3-*R***, H atoms, hydroxide anions and lattice hydrate molecules are not shown for clarity.

Table S2. Continuous Shape Measures calculation for Dy1 atom in **4-*S***.

Dy1 structures

EP-9	1 D9h	Enneagon
OPY-9	2 C8v	Octagonal pyramid
HBPY-9	3 D7h	Heptagonal bipyramid
JTC-9	4 C3v	Johnson triangular cupola J3
JCCU-9	5 C4v	Capped cube J8
CCU-9	6 C4v	Spherical-relaxed capped cube
JCSAPR-9	7 C4v	Capped square antiprism J10
CSAPR-9	8 C4v	Spherical capped square antiprism
JTCTPR-9	9 D3h	Tricapped trigonal prism J51
TCTPR-9	10 D3h	Spherical tricapped trigonal prism
JTDIC-9	11 C3v	Tridiminished icosahedron J63
HH-9	12 C2v	Hula-hoop
MFF-9	13 Cs	Muffin

Structure [ML9]	EP-9	OPY-9	HBPY-9	JTC-9	JCCU-9	CCU-9	JCSAPR-9	CSAPR-9	JTCTPR-9	TCTPR-9	JTDIC-9	HH-9	MFF-9
ABOXIY	33.232	22.068	17.306	15.642	10.001	8.784	4.976	4.295	6.460	5.015	13.071	6.894	**3.400**

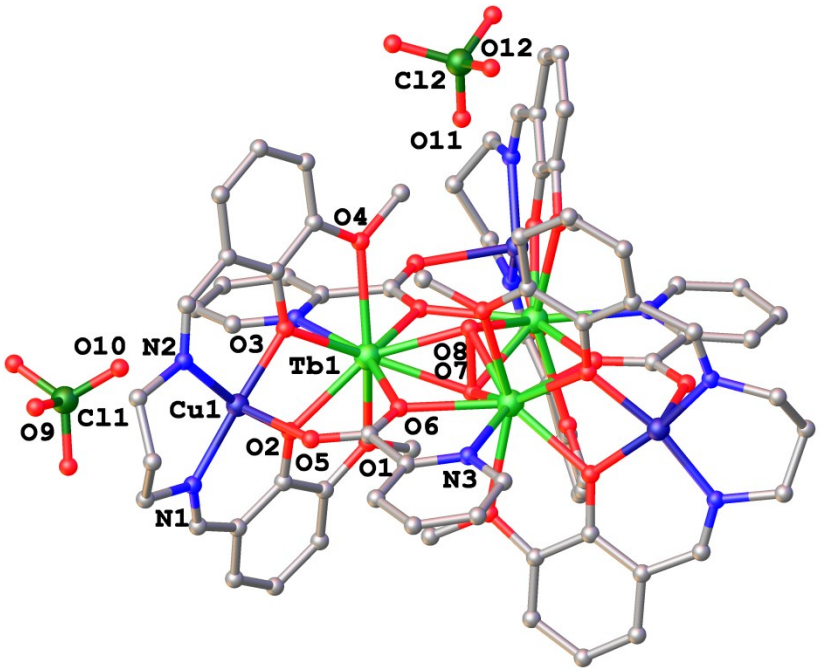

Fig. S7. Crystal structure of **5-*S***, H atoms, hydroxide anions and lattice hydrate molecules are not shown for clarity.

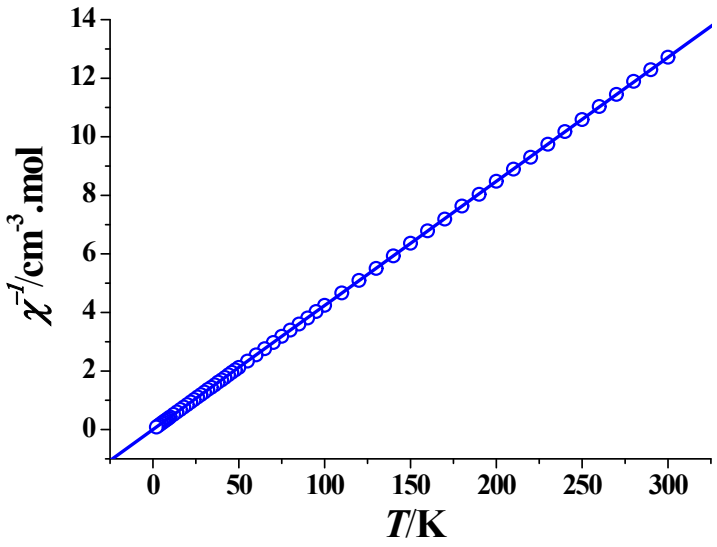

Fig. S8. Plot of $1/\chi$ *versus* T for **3** (H_{dc} = 1000 Oe).

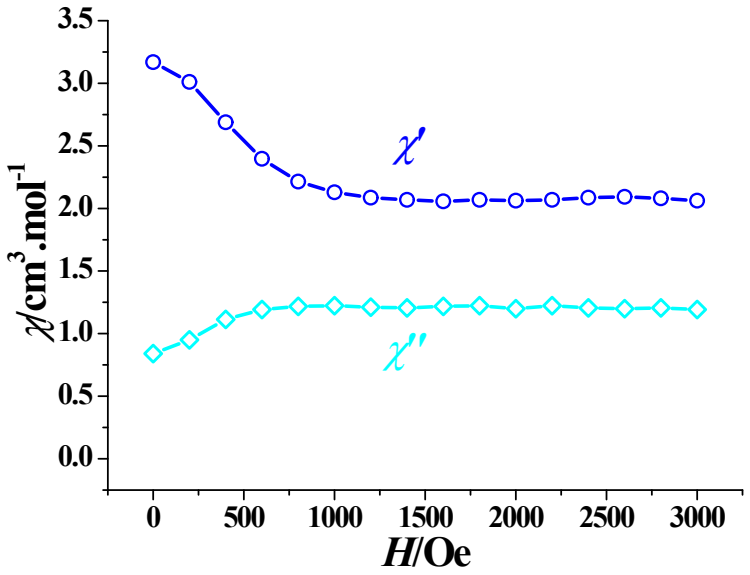

Fig. S9. AC susceptibilities measured at 2.5 Oe ac magnetic field with variable dc fields at 997 Hz and 10.5 K for **1**.

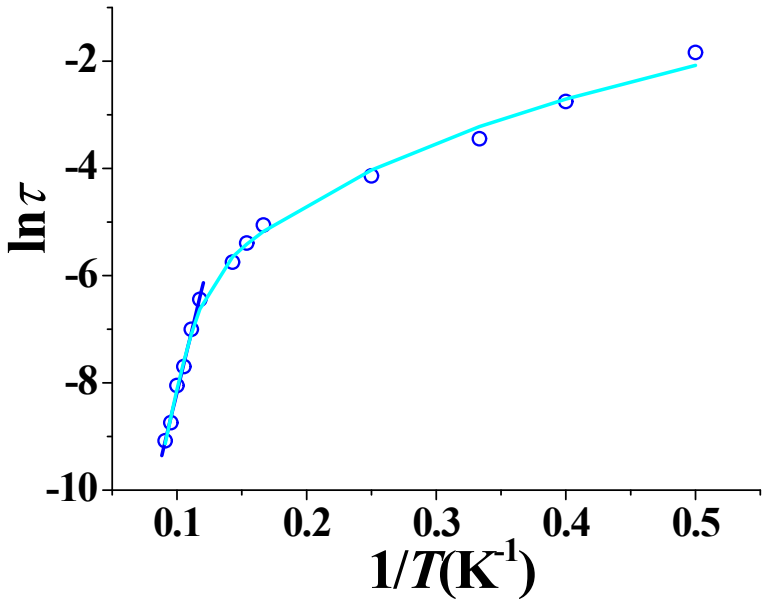

Fig. S10. Plot of ln(τ) *versus* 1/T for **1** (H_{dc} = 1000 Oe). The solid lines represent the best fitting with the Arrhenius law (blue) and Orbach *plus* Raman (cyan).

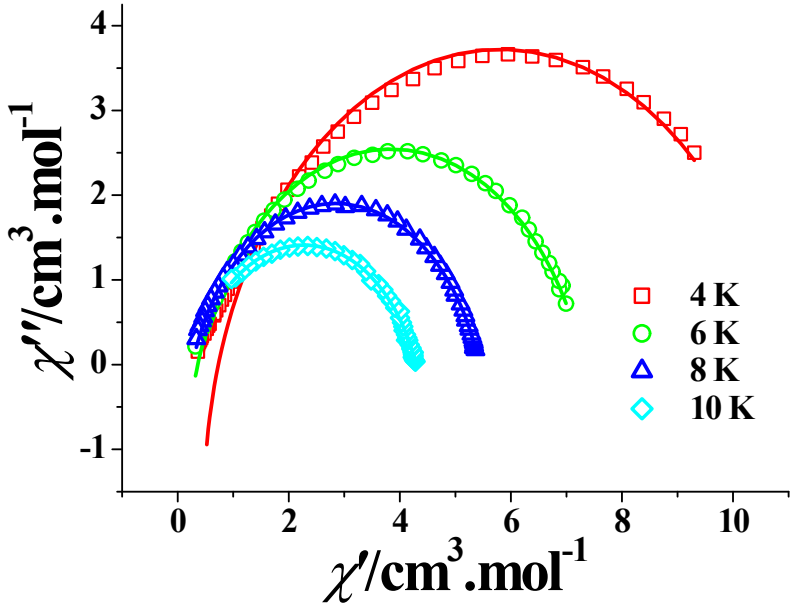

Fig. S11. Cole-Cole plots at 4-10 K for **1** (H_{dc} = 1000 Oe and H_{ac} = 2.5 Oe), the solid lines represent the best fitting.

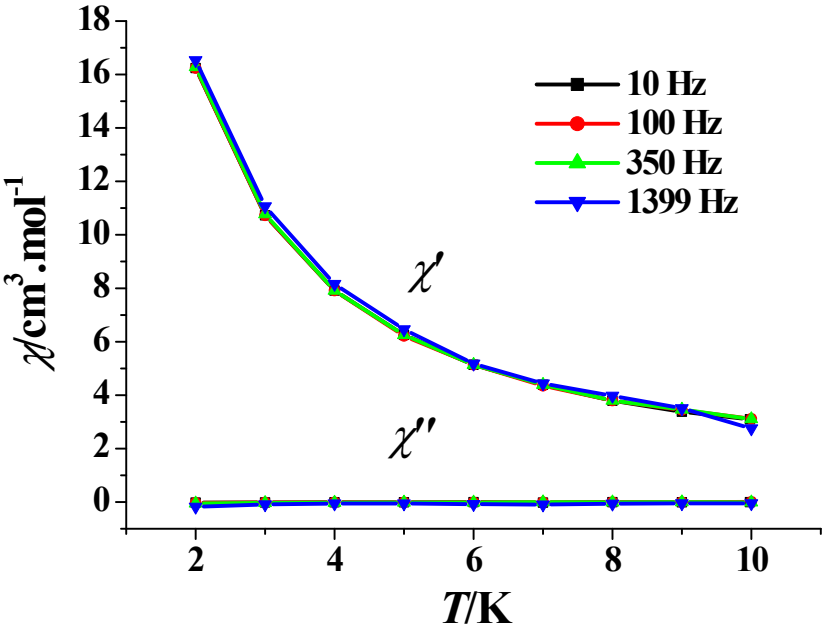

Fig. S12. AC susceptibilities for **2** (H_{dc} = 0 Oe and H_{ac} = 2.5 Oe).

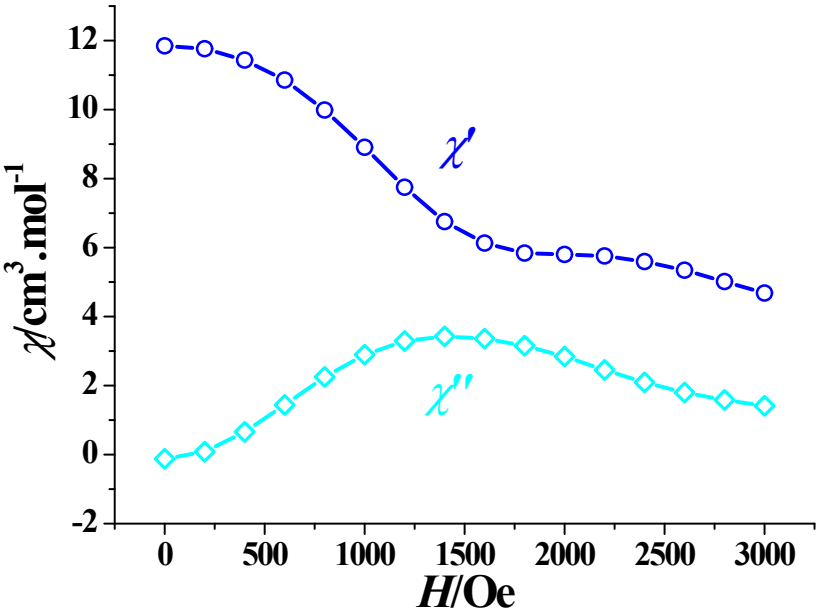

Fig. S13. AC susceptibilities measured at 2.5 Oe ac magnetic field with variable dc fields at 997 Hz and 3 K for **2**.

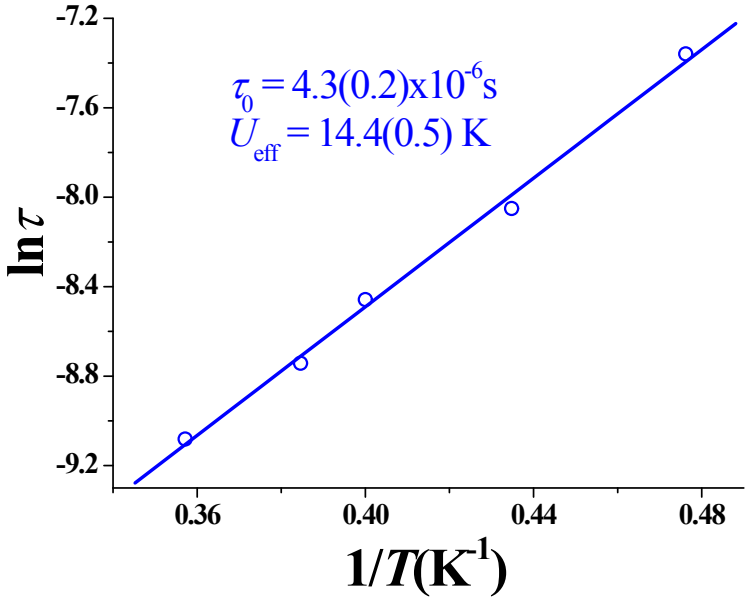

Fig. S14. Plot of ln(τ) *versus* 1/*T* for **2** (H_{dc} = 1400 Oe), the solid line represents the best fitting with the Arrhenius law.

Table S3. Linear combination of two modified Debye model fitting parameters from

1.9 K to 3.1 K of **2** under 1400 Oe dc field.

T(K)	χ_2(cm^3.mol^{-1})	χ_1(cm^3.mol^{-1})	χ_0(cm^3.mol^{-1})	τ_1(s)	α_1	τ_2(s)	α_2
1.9	14.8869	7.65154	2.84358	0.08422	0.09757	0.00021	0.09033
2.2	13.5975	6.18693	2.58835	0.0821	0.17129	0.0002	0.06666
2.5	12.4808	5.04745	2.36233	0.0963	0.24692	0.00017	0.05196
2.8	11.4484	4.10277	2.16193	0.1044	0.28194	0.00015	0.04551
3.1	10.4721	3.36066	1.98698	0.10874	0.37049	0.00013	0.03844

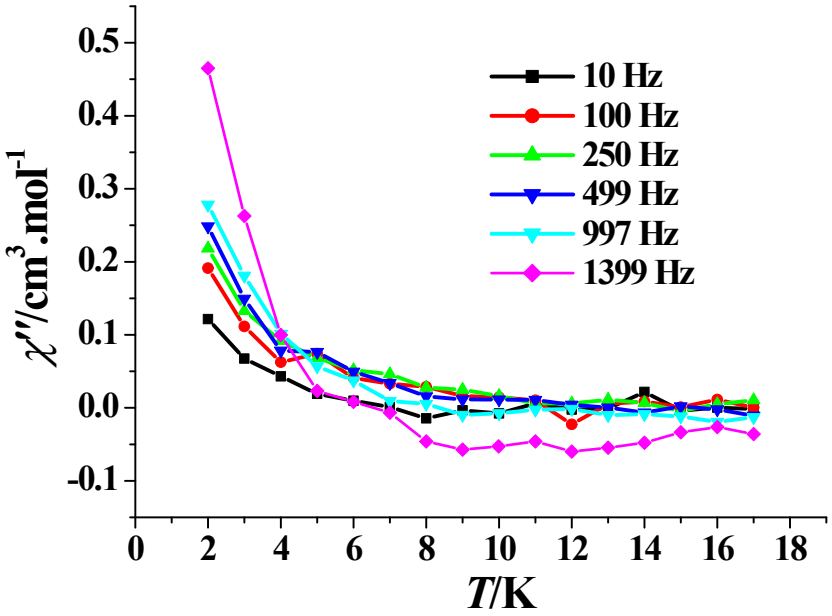

Fig. S15. Plots of χ'' *versus* T for **4** (H_{dc} = 0 Oe, H_{dc} = 0 Oe).

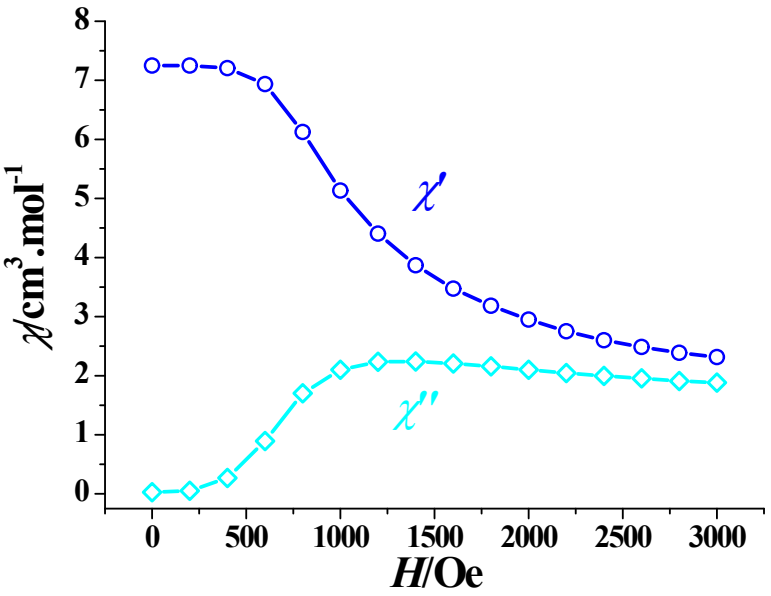

Fig. S16. AC susceptibilities measured at 2.5 Oe ac magnetic field with variable dc fields at 997 Hz and 7 K for **4**.

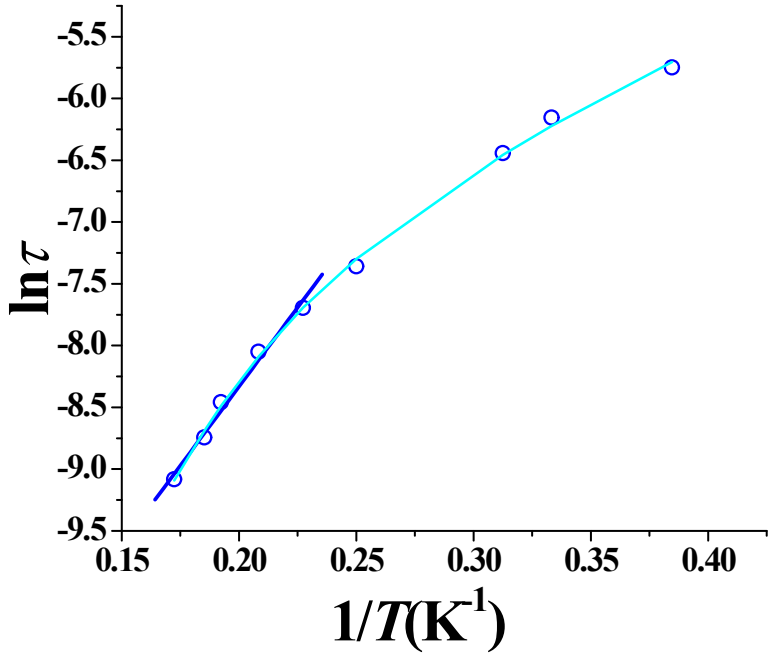

Fig. S17. Plot of ln(τ) *versus* 1/T for **4** (H_{dc} = 1400 Oe). The solid lines represent the best fitting with the Arrhenius law (blue) and Orbach plus Raman (cyan).

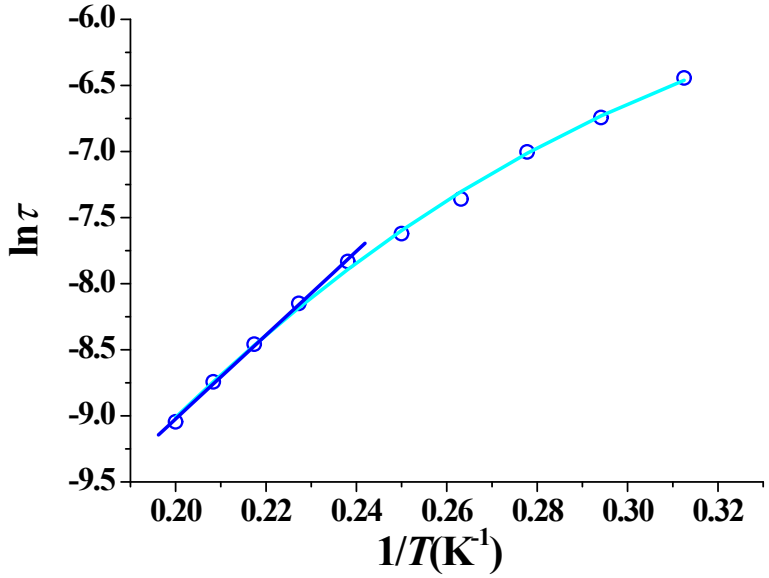

Fig. S18. Plot of ln(τ) *versus* 1/T for **5** (H_{dc} = 0 Oe). The solid lines represent the best fitting with the Arrhenius law (blue) and Orbach plus Raman and quantum tunneling effect (cyan).

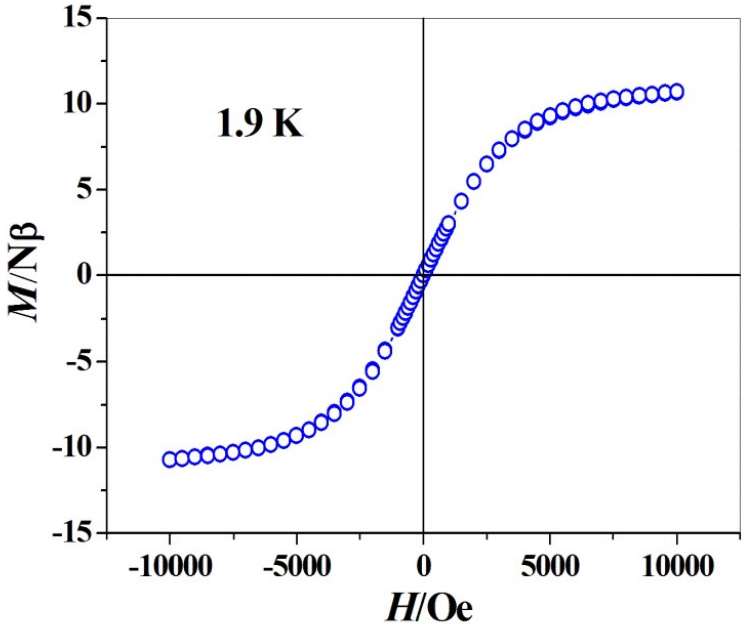

Fig. S19. Hysteresis loop for **5** at 1.9 K.